Electron Temperature Measurement by Thomson Scattering in Tokamak NOVA II

AUTHOR(S):

MASAMUNE, Sadao; YOKOYAMA, Issei; FUKAO, Masayuki; NISHIHARA, Hiroshi

CITATION:

MASAMUNE, Sadao ...[et al]. Electron Temperature Measurement by Thomson Scattering in Tokamak NOVA II. Memoirs of the Faculty of Engineering, Kyoto University 1982, 44(4): 451-459

ISSUE DATE:

1982-12-28

URL:

http://hdl.handle.net/2433/281225

Electron Temperature Measurement by Thomson Scattering in Tokamak NOVA II

By

Sadao MASAMUNE*, Issei YOKOYAMA**,
Masayuki FUKAO and Hiroshi NISHIHARA

(Received May 6, 1982)

Abstract

The Thomson scattering method was applied to determine the temperature and density profiles of plasma electrons in the NOVA II tokamak. To minimize the intensity of stray light, use was made of a viewing damp, which was an array of blue-glass knife edges.

The radial profile of electron density has been found to be approximately parabolic, while the temperature profile appeared more peaky and can be represented by the square of the parabolic expression. The electron energy confinement time determined by this method is in good agreement with that predicted by the Alcator scaling law.

§1. Introduction

The temperature and density of electrons in a high temperature plasma can be determined by means of the Thomson scattering of laser light.[1-5] This technique provides time- and space-resolved distributions with a sufficient accuracy, on the condition that the apparatus is designed properly. In the case of tokamak plasma, the electron density is low and, what is still worse, the intensity of the background radiation is high. Therefore, the Thomson scattering apparatus for a tokamak machine has to be designed carefully, so that there will be no unfavourable experimental conditions.

We can alternatively determine either the electron temperature T_e or the ion temperature T_i from an analysis of the spectrum of the Thomson scattering. The alternative is mainly controlled by the parameter $\alpha=[4\pi\lambda_D \sin(\theta/2)]^{-1}\lambda_L$, where θ is the angle between the incident and scattered beams, λ_D the Debye length and λ_L the wave length of the incident laser light. For $\alpha \lesssim 0.1$ and for $\alpha \gtrsim 1$, the scattering process is incoherent and coherent, respectively. The scattering of

Department of Nuclear Engineering
* Present address: Department of Electrical Engineering, Kyoto Technical University.
** Present address: Horiba Co., Ltd.

the visible laser radiation is incoherent when observed at $\theta=90°$. For electron temperatures below 1 keV, the spectrum of the Thomson scattering is approximately Gaussian, and in a particular case of the Ruby laser, the half width is

$$\Delta\lambda(\mathrm{FWHM}) = 32.5\sqrt{T_e}\,, \tag{1}$$

where $\Delta\lambda$ is in Å and T_e in eV. The electron temperature T_e is directly determined from Eq. (1) by using the observed width of the scattering spectrum.

In the case of incoherent scattering, the total intensity of the scattered light is given by

$$I = \frac{I_0}{S} n_e S l \frac{\mathrm{d}\sigma}{\mathrm{d}\Omega} \Delta\Omega\,, \tag{2}$$

where I_0 is the intensity of incidence, S the cross section of the incident beam, l the path length of the beam in the plasma column, $\mathrm{d}\sigma/\mathrm{d}\Omega$ the differential cross section for the Thomson scattering, $\Delta\Omega$ the solid angle of the collecting lens, respectively. In designing the apparatus, the F-numbers must be matched between the monochromator and the collecting lens. The matching condition is given by

$$\frac{h}{l} = \frac{\mathrm{F}_1}{\mathrm{F}_0}\,, \tag{3}$$

where h is the height of the monochromator slit, F_1 and F_0 are the F-numbers for the monochromator and the collecting lens, respectively. By using this matching condition in Eq. (2), it yields

$$I = \frac{\pi}{4} I_0 n_e \frac{\mathrm{d}\sigma}{\mathrm{d}\Omega} \frac{h}{\mathrm{F}_0\mathrm{F}_1}\,. \tag{4}$$

In this expression, the ratio $h/(\mathrm{F}_0\mathrm{F}_1)$ is the light collecting capacity of the apparatus. We have chosen $h=1$ cm and $\mathrm{F}_0=\mathrm{F}_1=4.5$.

This report describes the characteristics of the Thomson scattering apparatus for the NOVA II tokamak[6] and the obtained results.

§2. Apparatus

Figure 1 shows a schematic layout of the Thomson scattering apparatus built recently for determining the electron temperature and density in the NOVA II. The giant pulse Ruby laser consists of an oscillator, a Q-switch and an amplifier. Helical Xenon flash lamps are used in the oscillator and the amplifier, and a KD*P pockel cell in the Q-switch. A stable pulsed beam is fired with a 20 ns pulse width, and the maximum energy is 12 J. The beam divergence is less than 3 mrad. The horizontal laser beam is sent vertically up into the machine through

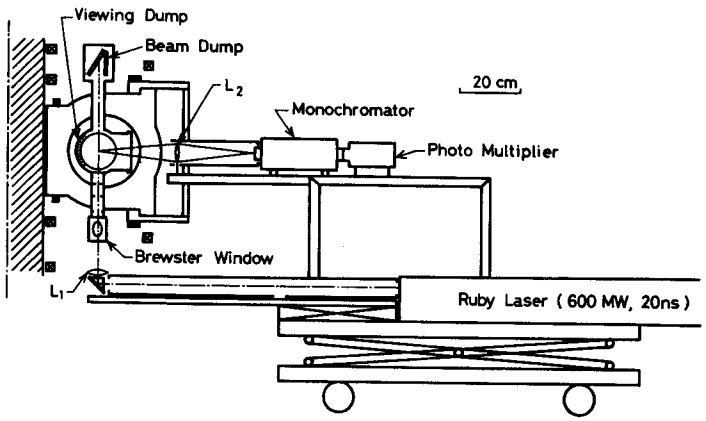

Fig. 1. Schematic drawing of the Thomson scattering apparatus.

a rectangular prism. The lens L_1 with a 40 cm focal length focusses the beam to a spot, 2 mm in diameter. The plasma is scanned vertically by moving the spot. The window for the beam incidence is fixed at the Brewster angle, with respect to the beam axis, in order to avoid excessive energy concentration on the window surface. The beam damp consists of two blue-glass plates, one of which is again fixed at the Brewster angle.

The scattered light is collected by the lens L_2 having a 56 mm diameter. To minimize the background due to stray light, a viewing damp is attached to the inner wall of the discharge chamber so that it covers that part of the wall where the aperture of the monochromator is visible. We have tested three types of viewing damps; i) stainless steel knife edges, 0.5 mm thick, separated by 0.5 mm from each other, ii) stainless steel knife edges arranged closely, and iii) an array of blue-glass knife edges, having a 2 mm thickness, fixed closely. The reflection coefficient was measured with the instrumentation shown in Fig. 2 (a). The viewing damp was exposed to a helium-neon laser beam incident at an angle θ to the optical axis of the collector photo-multiplier. The relative intensity of reflection is shown in Fig. 2 (b) as a function of the angle θ. This figure clearly shows that the blue-glass viewing damp is the best among those tested. The knife edges are exposed to scrape-off layer plasmas whose typical parameters are $n_e \simeq 10^{12}$ cm^{-3} and $T_e \simeq 20$ eV. Nevertheless, no appreciable damage of the edges was detected.

The scattered light is collected by the lens L_2, 56 mm in diameter, and is detected by a photo-multiplier tube (HTV R-943). The monochromator is a 25 cm Czerney-Turner mount which has a 52 mm $\times$ 52 mm grating with a dispersion of 30 Å/mm. Both the entrance and exit slits are 10 mm high and 1 mm wide. Therefore, the channel width is 30 Å per channel. Single-channel spectrum analy-

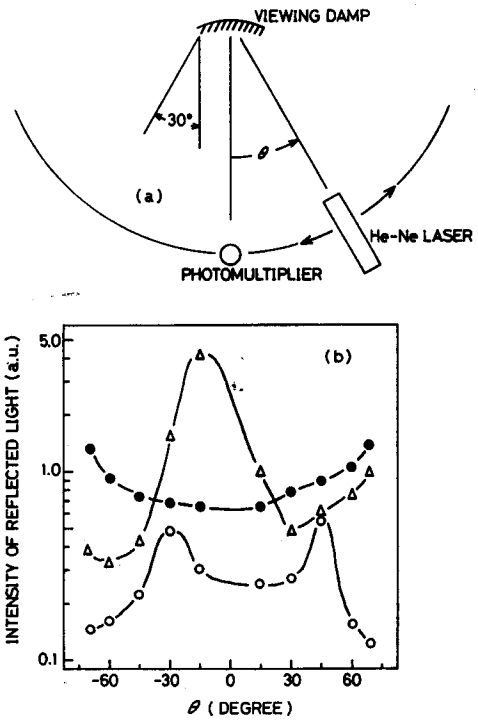

Fig. 2. (a) Instrumentation for the measurement of angular distribution of reflection factors for three types of viewing damps. (b) Angular distribution of reflection factors. Triangle: stainless steel knife edges arranged separately at a distance of 0.5 mm; Filled circle: stainless steel knife edges arranged closely; Open circle: blue-glass knife edges arranged closely.

ses were performed for central wave lengths of 6813, 6750, 6720, 6660, 6610 and 6520 Å. The photo-multiplier tube has a square photo-cathode (10 mm × 10 mm) of GaAs with a high quantum efficiency in the red and near infra-red regions. The tube is shielded from the strong magnetic field of the tokamak machine by means of a 3 mm soft iron housing plus a μ-metal shield, 1 mm thick.

§3. Experiments

The measurement of the electron temperature and density by the Thomson scattering method has been performed on the plasma of the NOVA II tokamak, whose major and minor radii, R and a, are 30 and 6 cm, respectively. The experimental arrangement is schematically shown in Fig. 3. The impurity ions are suppressed and the gas recycling is controlled by the techniques of both titanium

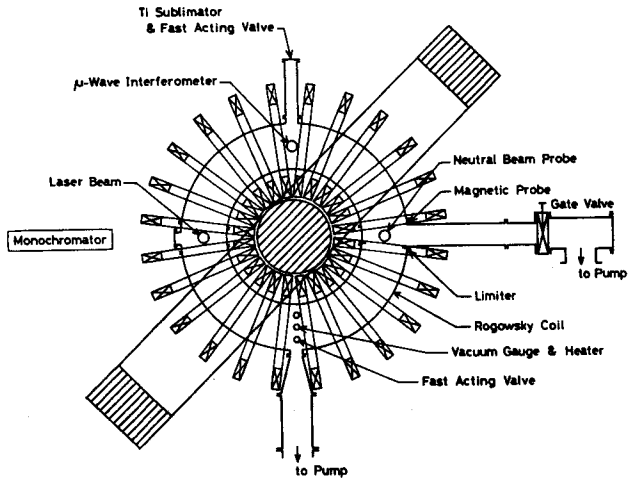

Fig. 3. Experimental arrangement.

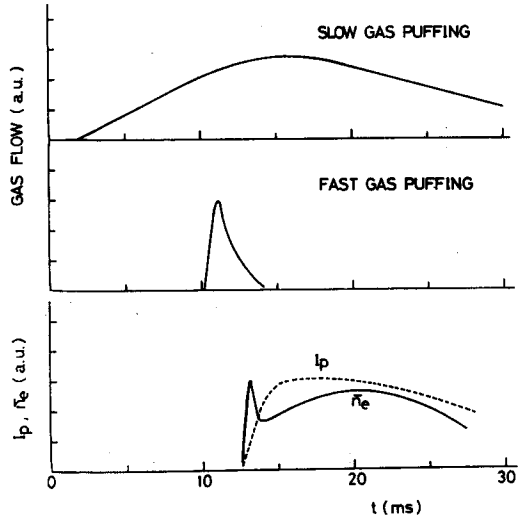

Fig. 4. Time sequence of gas puffing.

gettering and gas puffing. The time sequence of the gas puffing is digramatically shown in Fig. 4. A slow gas injector is started about 10 ms before the ignition of the discharge. In addition to this, a fast injector is worked 2 ms before the ignition. The plasma density is maintained during the discharge by slow gas puffing. Fast gas puffing reduces the production of runaway electrons, and suppresses the interaction between the plasma and the limiter in the current rise stage. Fast gas puffing immediately followed by ignition is effectual for obtaining a stable high-density plasma.[8,9] The toroidal field intensity was typically 1.0 T throughout the

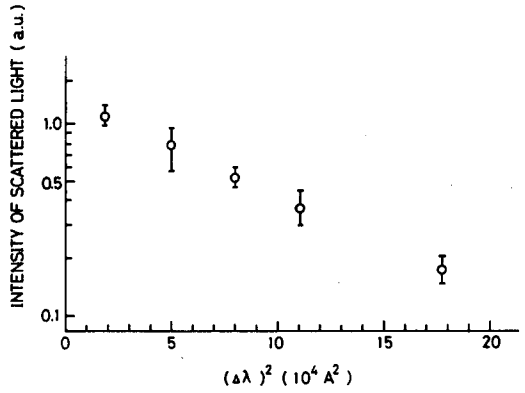

Fig. 5. Typical spectrum of the scattered Ruby laser light.

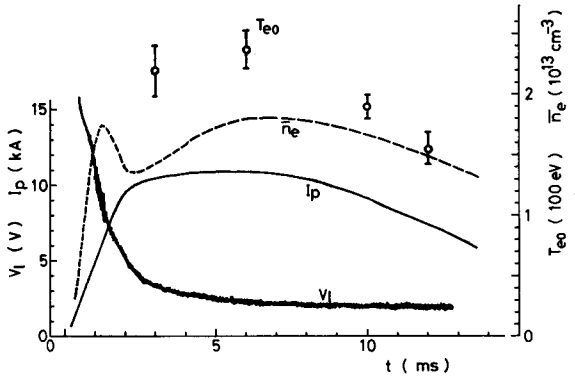

Fig. 6. Time behaviros of the loop voltage V_l, the plasma current I_p, the average density $\bar{n}_e$, and the central electron temperature $T_e(0)$.

experiment.

An example of the observed spectra of the Thomson scattering method is shown in Fig. 5. The spectrum measurement was performed in the quasi-steady state at 6 ms after the ignition. Each of the open circles is the average of 5 to 10 observations, while the bars show the standard deviations. The electron temperature T_e was obtained by the least-square fit of the Gaussian distributions to the observed spectra. To establish a spectrum and its temperature, 40 to 60 shots of the discharge were tried. The electron density n_e was simultaneously determined by means of the measurement of the total intensity of Thomson scattering and the microwave interferometry.

Figure 6 shows the typical time behaviors of the loop voltage V_l, the plasma current I_p, the line-averaged electron density $\bar{n}_e$ by a 6-mm microwave interferometer, and the central electron temperature $T_e(0)$. In this figure, the fast

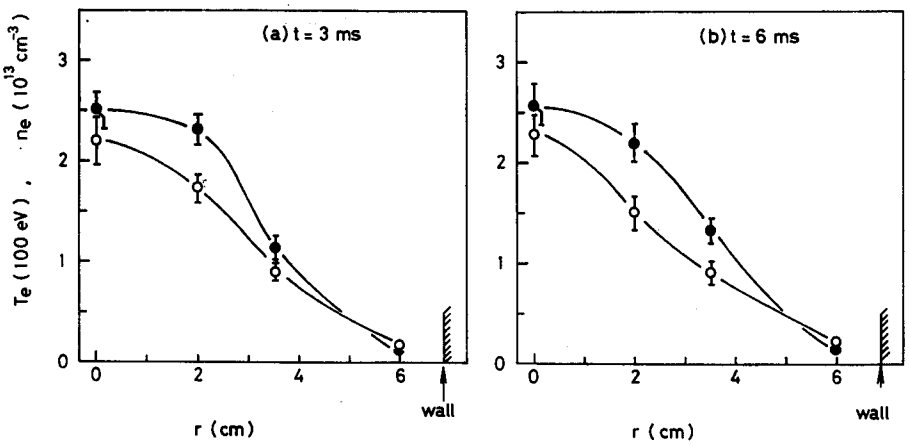

Fig. 7. Typical radial profiles of electron temperature and density measured at $t=3$ and 6 ms after the start of discharge.

initial rise of the initial density is followed by a rapid decay. The peak value indicates that the initial filling gas is ionized by half. The rapid decay of electron density is stopped, because the gas pressure is recovered by slow gas puffing, and the average density reaches a wide second peak.

Figure 7 shows the radial profiles of the electron temperature $T_e(r)$ and density $n_e(r)$ at 3 and 6 ms after the ignition of the discharge. Near the plasma boundary, both the temperature and density were measured by the method of electrostatic probing. Reasonable expressions of the observed temperature and density profiles are as follows:

$$T_e(r) = [T_e(0) - T_e(a)]\,[1-(r/a)^2]^2 + T_e(a)\,, \qquad (5)$$

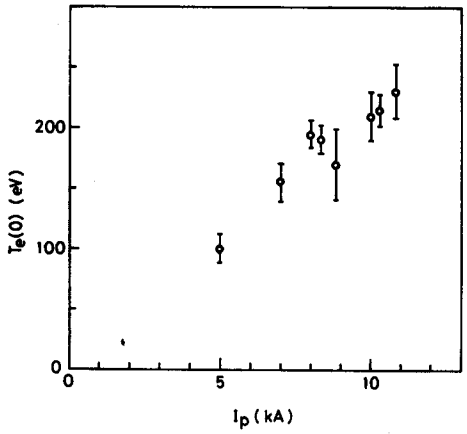

Fig. 8. The central electron temperature $T_e(0)$ versus the plateau value of the plasma current I_p.

$$n_e(r) = [n_e(0) - n_e(a)][1-(r/a)^2] + n_e(a) \,. \qquad (6)$$

Figures 6 and 7 show that the temperature profile is established in the earlier stage of discharge, and remains almost unchanged for several milliseconds.

Figure 8 shows the central electron temperature $T_e(0)$ in the quasi-steady state for the plateau values of the plasma current I_p from 5 to 11 kA. The temperature increases almost linearly up to 250 eV with an increased plasma current.

By using the radial profiles of the electron temperature and density, we can estimate the global electron energy confinement time τ_E^e defined by

$$\tau_E^e = \frac{4\pi^2 R\int \frac{3}{2} n_e T_e r dr}{P_{OH}} \simeq \frac{4\pi^2 R\int \frac{3}{2} n_e T_e r dr}{V_l I_p} \,, \qquad (7)$$

where P_{OH} is the power of Ohmic heating. In the quasi-steady state, P_{OH} is approximately equal to the plasma current I_p multiplied by the loop voltage V_l at the position of the conducting shell. Figure 9 shows the confinement time versus the average density $\bar{n}_e$. The average density varied from 1×10^{13} to 2.4×10^{13} cm^{-3}, while the current was kept around 10 kA. The confinement time τ_E^e increases with an increased electron density. This is because the electron temperature is mainly determined by the plasma current. By assuming $T_e/I_p \simeq$constant in Eq. (7), it immediately yields the relation $\tau_E^e \propto \bar{n}_e$.

The Alcator scaling law[10] is

$$\tau_{E,Al} = \alpha a^2 n_{14} \,, \qquad (8)$$

where a is the minor radius in m, and n_{14} the line-averaged density in 10^{14} cm^{-3}. The coefficient α takes on a value between 0.6 and 1.0. In Fig. 9, the extreme cases of this scaling law for $\alpha=0.6$ and $\alpha=1.0$ are shown for comparison. It

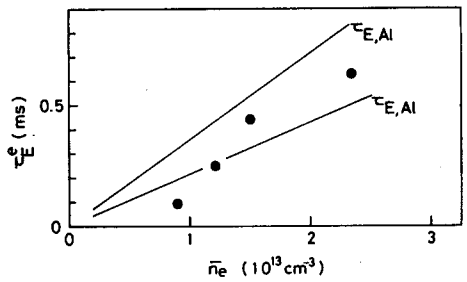

Fig. 9. The global electron energy confinement time τ_E^e versus the average density $\bar{n}_e$. $\tau_{E,Al}$ is the energy confinement time expected from the so called Alcator scaling law for the two cases of the numericl coefficients of 0.6 and 1.0.

should be noted that Fig. 9 indicates the consistency of the NOVA II confinement time with the established Alcator scaling law for tokamak plasmas.

§4. Summary

The Thomson scattering method was applied to determine the temperature and density profiles of plasma electrons in the NOVA II tokamak. The results obtained are summarized as follows:

1) Use was made of a viewing damp, which was an array of blue-glass knife edges. It was the most effective as regards minimizing the intensity of stray light among the three types of viewing damps tested, including two types of widely used viewing damps of stainless steel knife edges.

2) The radial profile of the electron temperature has been found to be approximately the square of the parabolic expression, while the density profile appeared somewhat broader and can be represented by the parabolic expression.

3) The global electron energy confinement time determined from the temperature and density profiles is in good agreement with that predicted from the Alcator scaling law.

Acknowledgment

The authors wish to thank Drs. H. Zushi and K. Kondo of the Plasma Physics Laboratory, Kyoto University, for their valuable information and useful discussions.

References

1) M. J. Forrest, N. J. Peacock, D. C. Robinson, V. V. Sannikov and P. D. Wilcock: *Culham Laboratory Report*, CLM-R 107 (1970).
2) J. S. Culver and M. Murakami: *Proc. 5th Symp. Eng. Problems of Fusion Res.*, Princeton University (1973).
3) M. Charet, L. Dumey, C. DeMichelis and P. Platz: *Association Euratom-CEA, Fontenay-aux-Roses Report*, EUR-CEA-FC 759 (1975).
4) T. Matoba, A. Funahashi and K. Ando: *Japan Atomic Energy Research Institute Report*, JAERI-M 5515 (1973).
5) K. Kawahata, Y. Hamada, A. Yasuda and K. Miyamoto: Jpn. J. Appl. Phys. **18** 627 (1979).
6) M. Fukao, Y. Fujiwara, H. Zushi, H. Sumeitsu et al.: Mem. Fac. Eng., Kyoto Univ. **39** 431 (1977).
7) J. Sheffield: *Plasma Scattering of Electromagnetic Radiation*, (Academic Press, London, 1975).
8) R. J. Hawryluk, K. Bol, N. Bretz, D. Dimock et al.: Nucl. Fusion **19** 1307 (1979).
9) R. S. Granetz, I. H. Hutchinson and D. O. Overskei: Nucl. Fusion **19** 1587 (1979).
10) W. Pfeiffer and R. E. Waltz: Nucl. Fusion **19** 51 (1979).